Spatial Duty Cycle Model for Cognitive Radio

Miguel López-Benítez and Fernando Casadevall
Department of Signal Theory and Communications
Universitat Politècnica de Catalunya (UPC)
Barcelona, Spain
Email: {miguel.lopez, ferranc}@tsc.upc.edu

***Abstract*—Spectrum occupancy modeling in the context of Dynamic Spectrum Access/Cognitive Radio (DSA/CR) constitutes a rather unexplored research area that still requires much more effort. This paper addresses the problem of modeling spectrum occupancy in the spatial domain by proposing a novel theoretical approach that enables modeling the occupancy level perceived at any geographical location based on the knowledge of some simple primary signal parameters. The validity of the theoretical model is verified with extensive empirical measurement results. Some examples of its potential applicability are discussed as well.**

I. Introduction

The dramatic spectrum demand growth experienced during the last years has resulted in the so-called *spectrum scarcity problem*. Recent spectrum measurement campaigns [1–6] have demonstrated, however, that spectrum is vastly underutilized and the virtual scarcity actually results from the fixed and inflexible spectrum access policies currently employed in most regulatory regimes. This situation has motivated the emergence of Dynamic Spectrum Access (DSA) policies based on the Cognitive Radio (CR) technology [7]. The basic underlying principle of DSA/CR is to allow unlicensed users to access in an opportunistic and non-interfering manner some licensed bands temporarily unoccupied by the licensed users. Unlicensed (secondary) CR terminals sense the spectrum to detect spectrum gaps left by licensed (primary) users and transmit on them. Secondary unlicensed transmissions are allowed following this operating principle as long as they do not provoke harmful interference levels to the primary network.

Due to the opportunistic nature of the DSA paradigm, the behavior and performance of a secondary CR network strongly depends on the spectrum occupancy patterns of the primary networks. A realistic and accurate modeling of such patterns becomes therefore essential and extremely useful in the domain of DSA/CR research. The potential applicability of spectrum use models ranges from analytical studies to the design and dimensioning of secondary networks, including the development of innovative simulation tools as well as novel DSA techniques. Nevertheless, the utility of such models depends on their realism and accuracy degree. Unfortunately, the models for spectrum use commonly used to the date in DSA/CR research are limited in scope and based on oversimplifications or assumptions that have not been validated with empirical measurement data. Spectrum occupancy modeling in the context of DSA/CR constitutes a rather unexplored research area that still requires much more effort.

In this paper we address the problem of modeling spectrum occupancy in the spatial domain. Previous works in this area have faced the problem from a statistical perspective. In [8], some methods of spatial statistics are employed to evaluate the variability and correlation of spectrum occupancy among sectors of a mobile communication cellular system based on measurements of a real network. In [9], the theories of random fields and point processes are employed to model the Power Spectral Density (PSD) distribution over space. Both techniques have successfully been applied to selected problems in wireless communications before. In this paper we introduce a novel spatial spectrum use model based on a different, simple, clear and intuitive theoretical approach that enables modeling the occupancy level perceived at any geographical location based on the knowledge of some simple primary signal parameters. The validity and correctness of the theoretical model developed in this work is evaluated and corroborated with extensive empirical measurement results for various frequency bands and radio technologies.

The rest of this paper is organized as follows. First, section II presents the measurement setup and scenario considered in this work. Sections III, IV and V discuss some preliminary issues required for the development of the theoretical model presented in section VI. The potential applications of the model proposed in this work are discussed and exemplified in section VII. Finally, section VIII concludes the paper.

II. Measurement Setup and Scenarios

The measurement configuration employed in this work (see Figure 1) relies on a spectrum analyzer setup where different external devices have been added in order to improve the detection capabilities and hence obtain more accurate and reliable results. The design is composed of two broadband discone-type antennas covering the frequency range from 75 to 7075 MHz, a Single-Pole Double-Throw (SPDT) switch to select the desired antenna, several filters to remove undesired overloading (FM) and out-of-band signals, a low-noise preamplifier to enhance the overall sensitivity and thus the ability to detect weak signals, and a high performance spectrum analyzer to record the spectral activity. A detailed description of the measurement setup design and configuration principles as well as the methodological procedures considered can be found in [10], where some important methodological aspects to be accounted for when evaluating spectrum occupancy in the context of CR are analyzed and discussed.

The measurement equipment of Figure 1 was employed to perform empirical measurements of various spectrum bands throughout the UPC campus in an urban environment in Barcelona, Spain. The different considered geographical locations are illustrated in Figure 2 and include both indoor (2) and outdoor environments at high points (1), narrow streets (3–7), between buildings (8–10) and in open areas (11–12). For more details, the reader is referred to [11]. The considered measurement locations represent various physical scenarios of practical interest and embrace a wide range of receiving conditions and levels of radio propagation blocking, ranging from direct line of sight to severely blocked and faded signals.

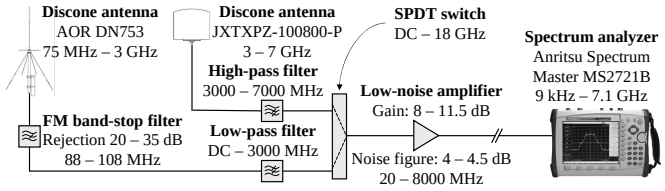

Fig. 1. Measurement setup employed in this study.

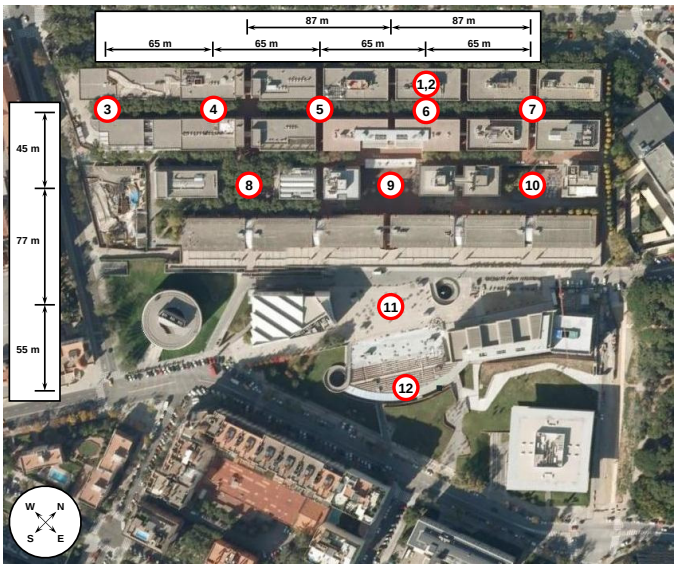

Fig. 2. Measurement locations considered in this study.

This variety of measurement conditions enabled us to observe the same set of transmitters under different propagation conditions and with different levels of Signal-to-Noise Ratio (SNR). The empirical data captured for various radio technologies at each location enabled an adequate validation of the theoretical model developed in this work.

III. Duty Cycle Definition

The model introduced in this work describes the spatial distribution of the Duty Cycle (DC). The DC can be defined from both empirical and probabilistic perspectives. From an empirical viewpoint, the DC can be defined as the fraction (or percentage) of time that a certain channel (or frequency range) is observed as occupied by a secondary CR terminal at a given geographical location. From a probabilistic viewpoint, the DC can be defined as the probability that a certain channel (or frequency range) is observed as occupied at a given geographical location. While the former is more appropriate for the validation with measurement results, the latter results more convenient for theoretical analyses.

The interest of employing the DC lies in its ability to summarize the overall spectrum occupancy within a certain time and frequency range in a single numerical value. The duty cycle has been employed in many past spectrum occupancy studies to quantify and compare the occupancy level of several spectrum bands, or to compare the occupancy of the same band under different conditions or at different locations. In this work we employ the DC spatial distribution as a mean to describe the spatial spectrum occupancy that would be perceived by a secondary CR terminal at different locations.

It is important to make a clear distinction between the Activity Factor (AF) of a primary transmitter in a certain channel and the DC perceived by a secondary CR terminal in that channel. The AF of a primary transmitter represents the fraction (or percentage) of time that the transmitter is active (i.e., transmitting in the channel). A CR terminal in an arbitrary location with good propagation conditions with respect to the primary transmitter would observe the channel as occupied whenever the primary transmitter is active. However, at other locations where the propagation conditions are not so favorable, the primary signal might not be detected. In such a case, the level of spectrum activity perceived by the CR terminal (i.e., the DC) would be lower than the actual AF of the primary transmitter. While the AF is unique for a given transmitter, the DC perceived at different locations may be different. Since the propagation conditions strongly vary with the geographical location, the perceived DC will vary over space accordingly. The aim of this work is to develop a model able to describe the spatial distribution of the DC as a function of the propagation conditions.

IV. Energy Detection

Before transmitting, a CR terminal has to determine whether a primary signal is present in the spectrum band of interest. Several signal detection principles, referred to as spectrum sensing schemes in the context of CR, have been proposed in the literature to perform such task [12, 13]. They provide different trade-offs between required sensing time, complexity and detection capabilities. Their applicability depends on how much information is available about the primary signal. In the most generic case, a CR user is not expected to be provided with any prior information about the primary signals that may be present within a certain frequency band. When the secondary receiver cannot gather sufficient information about the primary signal, the energy detection principle can be employed due to its ability to work irrespective of the actual signal to be detected. Due to its simplicity and relevance, energy detection has been a preferred approach for many past CR studies and also is the approach adopted in this study.

An energy detector measures the signal energy received in a certain frequency band during an specified time period and employs this value as a test statistic $\mathbb{T}$. The test statistic $\mathbb{T}$ is then compared to a predefined decision threshold λ. If the signal energy lies above the threshold ($\mathbb{T} > \lambda$), a licensed signal is declared to be present. Otherwise ($\mathbb{T} < \lambda$), the measured frequency channel is supposed to be idle. In practice, the decision threshold λ is normally chosen to satisfy a certain probability of false alarm, which is defined as the probability that the channel is declared to be occupied when it is actually free (for an energy detector, a false alarm occurs when the noise energy exceeds the decision threshold). Interestingly, this method provides some detection benefits with respect to other simple methods for establishing the energy decision threshold [10] and is the approach considered in this work.

Since the measurement device employed in this study (spectrum analyzer) provides PSD values in dBm units, and in order to simplify the validation process, in this work we employ, without any loss of generality, the received signal power expressed in dBm as a test statistic $\mathbb{T}$ for the energy detection principle instead of the received signal energy.

V. Received Average Power Distribution

To decide if a channel is occupied, a CR terminal employing energy detection averages the power received during a predefined time period $2T$, which can be expressed as:

$$P_R = \frac{1}{2T}\int_{-T}^{+T} P_R(t)\,dt \tag{1}$$

where $P_R(t)$ is the instantaneous power received by the CR terminal and P_R is the average power computed in order to decide if a primary signal is present in the sensed channel.

To develop our model we are interested in the Probability Density Function (PDF) of the average power P_R. We assume that the PDF of $P_R(t)$ is in general unknown since it is the result of the combined effects of the primary transmission power pattern, which in principle is unknown, and the propagation effects. However, we assume that the mean value of $P_R(t)$, denoted as $\mu_{R,t}$, and its variance, denoted as $\sigma^2_{R,t}$, can be computed at any arbitrary location by employing an appropriate propagation model (notice that this procedure is not restricted to any propagation model in particular).

The instantaneous power $P_R(t)$ is as a stochastic process that can be thought of as a non-countable infinity of independent and identically distributed random variables, one for each time instant t, with mean $\mu_{R,t}$ and variance $\sigma^2_{R,t}$. Since P_R is obtained as the average of an infinite number of random variables, the central limit theorem can therefore be employed to approximate the PDF of P_R as a normal distribution, regardless of the actual PDF of $P_R(t)$, with mean μ_R and variance σ^2_R given by [14, pp. 523–525]:

$$\mu_R = \mathrm{E}\{P_R\} = \frac{1}{2T}\int_{-T}^{+T}\mathrm{E}\{P_R(t)\}\,dt = \mu_{R,t} \tag{2}$$

$$\begin{aligned}\sigma^2_R &= \mathrm{Var}\{P_R\} = \frac{1}{T}\int_0^{2T} C_R(\tau)\left(1-\frac{\tau}{2T}\right)d\tau \\ &\approx \frac{1}{T}\int_0^{2T} C_R(\tau)\,d\tau \approx \frac{1}{T}\int_0^{\infty} C_R(\tau)\,d\tau \\ &\approx \frac{\tau_c}{T}\,C_R(0) = \frac{\tau_c}{T}\,\sigma^2_{R,t}\end{aligned} \tag{3}$$

where T has been assumed to be sufficiently large, $C_R(\tau)$ is the autocovariance of $P_R(t)$ and τ_c is a constant called the *correlation time*, which satisfies that $C_R(\tau) \approx 0$ for $\tau > \tau_c$ and is defined as the ratio [14, p. 389]:

$$\tau_c = \frac{1}{C_R(0)}\int_0^{\infty} C_R(\tau)\,d\tau \tag{4}$$

As it can be appreciated, the received average power distribution can be modeled as a Gaussian PDF. Its mean value equals the mean value of the instantaneous received power and its variance is directly related to the variance of the instantaneous power and depends on the sensing period and the primary signal's autocorrelation properties.

The validity of the Gaussian approximation is verified in Figure 3 for various radio technologies and also for the thermal noise's average power (measured by replacing the antenna with a matched load). It is worth noting that the PSD values provided by a swept spectrum analyzer (our measurement device) are obtained by tuning a narrowband filter to a set of frequency points during a fixed time period, thus causing some unavoidable averaging effect over the measured signal. Therefore, the PSD values provided by our measurement device reflect the averaging effect of equation 1. Figure 3 compares the P_R values captured by the spectrum analyzer at some selected channels and the Gaussian curve corresponding to the sample mean and sample variance of the signal. Although different radio technologies are expected to exhibit various instantaneous power patterns $P_R(t)$, Figure 3 indicates that the received average power P_R can be modeled as a Gaussian random variable for all cases regardless of the particular instantaneous power distributions.

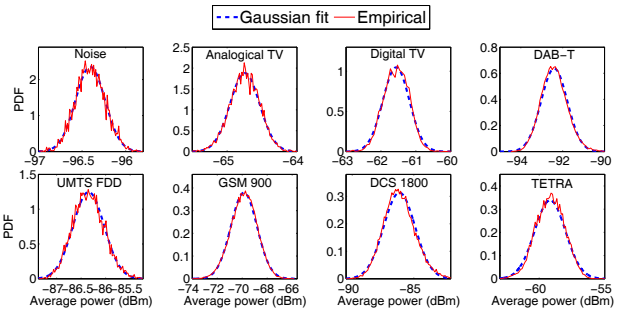

Fig. 3. Validation of the Gaussian approximation for the average power. The approximation is valid for line-of-sight measurements (location 1) and non-line-of-sight measurements (locations 2-12).

VI. Spatial Duty Cycle Model

A. Constant-Power Continuous Transmitters

In this section we focus on modeling the spectral occupancy, in terms of the DC, that would be perceived by a CR terminal at certain location for the particular case of constant-power transmitters with an AF of 100% (e.g., TV and DAB-T). This case provides the basis for a simple occupancy model that will be extended in the next sections for non-constant-power transmitters and/or discontinuous transmission patterns.

If the primary transmitter is always active, the PDF of the received average power, $f_R(P_R)$, will be that of the primary signal (with noise) at the location of the CR terminal, $f_S(P_S)$, which can be modeled as a Gaussian PDF with mean power μ_S and standard deviation σ_S. According to the probabilistic definition of section III, the DC, denoted as Ψ, can be computed as the probability that the received average power P_R is above the decision threshold λ (see Figure 4):

$$\begin{aligned}\Psi &= \int_\lambda^\infty f_R(P_R)dP_R = \frac{1}{\sqrt{2\pi}\sigma_S}\int_\lambda^\infty e^{-\frac{1}{2}\left(\frac{P_S-\mu_S}{\sigma_S}\right)^2}dP_S \\ &= \frac{1}{2}\,\mathrm{erfc}\left(\frac{\lambda-\mu_S}{\sqrt{2}\sigma_S}\right) = Q\left(\frac{\lambda-\mu_S}{\sigma_S}\right)\end{aligned} \tag{5}$$

where $\mathrm{erfc}(\cdot)$ is the complementary error function and $Q(\cdot)$ is the Gaussian Q-function.

As mentioned in section IV, the decision threshold λ is normally chosen to satisfy a certain probability of false alarm P_{fa}. Since average noise power can be modeled as a Gaussian law with mean μ_N and standard deviation σ_N (see Figure 4):

$$P_{fa} = \frac{1}{\sqrt{2\pi}\sigma_N}\int_\lambda^\infty e^{-\frac{1}{2}\left(\frac{P_N-\mu_N}{\sigma_N}\right)^2}dP_N = Q\left(\frac{\lambda-\mu_N}{\sigma_N}\right) \tag{6}$$

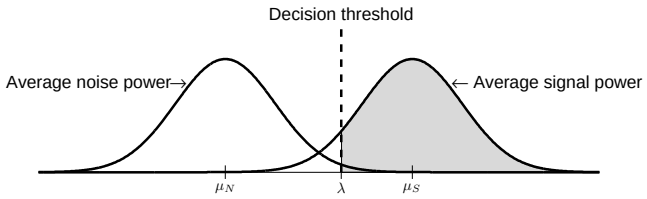

Fig. 4. Model considered for computing the duty cycle (shaded area).

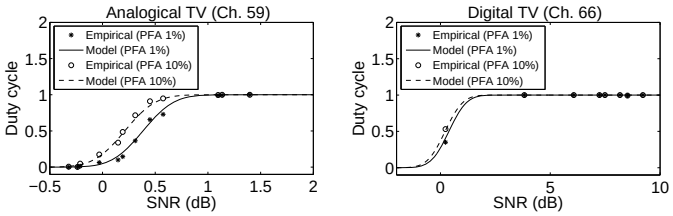

Fig. 5. Validation of DC model for constant-power continuous transmitters. Each empirical point corresponds to the result of one location in Figure 2.

Solving in equation 6 for λ yields the decision threshold:

$$\lambda = Q^{-1}(P_{fa})\ \sigma_N + \mu_N \tag{7}$$

where $Q^{-1}(\cdot)$ denotes the inverse of $Q(\cdot)$. Substituting equation 7 into equation 5 finally yields the DC model:

$$\Psi = Q\left(\frac{Q^{-1}(P_{fa})\ \sigma_N - \gamma}{\sigma_S}\right) \tag{8}$$

where $\gamma = \mu_S - \mu_N$ represents the average SNR expressed in decibels, while σ_S and σ_N are the standard deviation of the signal and noise average powers also in decibels.

To validate equation 8, Figure 5 depicts, for selected analogical and digital TV channels, the empirical DC obtained for the 12 locations measured in Figure 2. The empirical DC has been computed for the decision thresholds corresponding to P_{fa} = 1% and P_{fa} = 10%, and it is shown as a function of the difference between the empirically measured average signal power μ_S and average noise power μ_N in dBm, i.e. the SNR γ in dB. The dependence of the perceived spectral activity with the geographical location is reflected in the different SNR values observed at each location. The theoretical curve of equation 8 corresponding to the empirically measured means (μ_S,μ_N) and standard deviations (σ_S,σ_N) is also shown for comparison. As it can be appreciated, the model agrees with the empirical values for both analogical and digital channels. These results demonstrate that equation 8 is able to accurately predict the spectral activity that would be perceived by a CR user at any position based on some basic signal parameters.

B. Constant-Power Discontinuous Transmitters

In this section we extend the model of equation 8 by including the case of constant-power but non-continuous transmitters. If the primary transmitter is characterized by an AF $0 < \alpha < 1$, the PDF of the received average power, $f_R(P_R)$, will be that of the primary signal (with noise), $f_S(P_S)$, whenever the transmitter is active (which will occur with probability α), or thermal noise, $f_N(P_N)$, otherwise. Hence:

$$f_R(P_R) = (1-\alpha)\ f_N(P_N) + \alpha\ f_S(P_S) \tag{9}$$

and the resulting expression for the DC becomes:

$$\begin{aligned}
\Psi &= \int_\lambda^\infty f_R(P_R)dP_R \\
&= (1-\alpha)\int_\lambda^\infty f_N(P_N)dP_N + \alpha\int_\lambda^\infty f_S(P_S)dP_S \\
&= \frac{1-\alpha}{\sqrt{2\pi}\sigma_N}\int_\lambda^\infty e^{-\frac{1}{2}\left(\frac{P_N-\mu_N}{\sigma_N}\right)^2}dP_N + \\
&+ \frac{\alpha}{\sqrt{2\pi}\sigma_S}\int_\lambda^\infty e^{-\frac{1}{2}\left(\frac{P_S-\mu_S}{\sigma_S}\right)^2}dP_S \\
&= (1-\alpha)P_{fa} + \alpha\ Q\left(\frac{Q^{-1}(P_{fa})\ \sigma_N - \gamma}{\sigma_S}\right)
\end{aligned} \tag{10}$$

Notice that equation 8 is a particular case with $\alpha = 1$.

The validation of equation 10 based on the empirical measurements is not as straightforward as in section VI-A. While the values of μ_N and σ_N (receiver's noise) can be obtained by replacing the antenna with a matched load, the values of μ_S and σ_S cannot be obtained from the captured data sequences as in section VI-A because in the case of transmitters with $\alpha < 1$ the captured data is composed of both signal and noise samples, which cannot be distinguished reliably. Moreover, the actual AF of the transmitter, α, is also unknown and cannot reliably be derived from the measurements without additional information. To estimate μ_S, σ_S and α, we first compute the empirical PDF of the captured data sequences and employ curve-fitting procedures in order to fit equation 9, where μ_N and σ_N are known, to the empirical PDF. The set of values (μ_S, σ_S, α) minimizing the Root Mean Square Error (RSME) of the fit is then selected. As shown in Figure 6, the theoretical PDF corresponding to the empirically measured (μ_N, σ_N) and the estimated set (μ_S, σ_S, α) perfectly agrees with the empirical PDF, thus indicating that this procedure is able to provide good estimates of the true values. Applying these values to equation 10, the theoretical DC curve is obtained.

To obtain the empirical DC curve, it is important to notice that the locations considered in the measurement campaign were measured at different time instants and the actual AF during each measurement session might not be the same even for the same transmitter. When this occurs, the DC values obtained for each location/SNR are the result of different AFs and are therefore unrelated. As a result, the empirical curve obtained by plotting the empirical DC values as a function of the SNR is characterized by a completely random behavior. Since this phenomenon was observed in the empirical data sequences, a different approach was employed to obtain the empirical DC curve. The data sequence captured with the highest SNR was selected, and different SNR values were artificially emulated by subtracting the adequate amplitude value from all the samples of the original sequence. In a spectrum analyzer, signal amplitudes below the noise floor cannot be detected and are reported as noise. To emulate this effect, all the samples lying below the noise floor after subtracting the adequate amplitude value were replaced with the corresponding noise floor value. Moreover, the instantaneous noise floor value of a spectrum analyzer varies among sweeps. To emulate this effect, the noise floor sequence employed in this procedure was generated as a random variable drawn from a Gaussian distribution whose mean μ_N and standard deviation σ_N were obtained from the empirical measurements of the system's noise. The sequence obtained after this procedure was employed to compute the empirical DC for each SNR value. This procedure enables computing the DC corresponding to different SNR values for the same AF, and was proven to

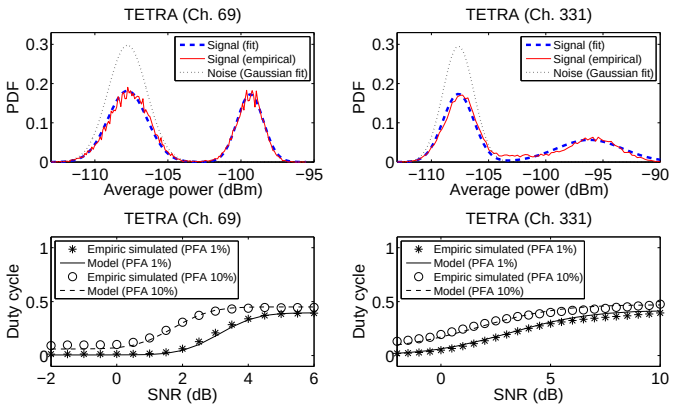

Fig. 6. Validation of the approach to estimate signal parameter's (upper part) and DC model for constant-power discontinuous transmitters (lower part).

provide realistic results. The DC curve obtained with this procedure, referred to as *empirical simulated*, is shown in Figure 6 and compared to the theoretical DC curve obtained as detailed above. As it can be appreciated, both curves agree, thus validating equation 10.

C. Variable-Power Discontinuous Transmitters

In this section the model is extended to account for variable-power transmitters. In this case, the average transmission power is not constant but characterized by a certain PDF. To simplify the model, let's assume that the variability of the transmission power can adequately be described by a discrete set of K average transmission power levels, instead of a continuous PDF. This assumption not only simplifies the analytical expressions of the model, but also enables the application of the model to the case in which a channel is time-shared by K transmitters with different power levels as it may be the case of various TDMA-based systems such as GSM/DCS, TETRA, etc. The model will be developed considering both cases, i.e. a single variable-power transmitter with K transmission power levels and K constant-power transmitters time-sharing the channel. In both cases, the problem reduces to the possibility of observing K different transmission powers in the channel.

Let's denote as $f_{S_k}(P_{S_k})$, with mean μ_{S_k} and standard deviation σ_{S_k}, the PDF of the received average power at certain location when the k-th transmission power level is present in the channel ($k = 1, 2, \ldots, K$). In general it can be assumed that $\mu_{S_p} \neq \mu_{S_q}$ and $\sigma_{S_p} \neq \sigma_{S_q}$ for $p \neq q$. Let's define an AF α_k for each transmission power representing the fraction of time (empirical definition) or the probability (probabilistic definition) that the k-th transmission power level is present in the channel. In the case of a single-transmitter with K transmission power levels, only one out of the K power levels can be selected at any time. Moreover, in the case of K transmitters time-sharing the channel it is reasonable to assume that there exists some Medium Access Control (MAC) mechanism so that when one primary transmitter accesses the channel the rest remain inactive. In both cases, the K average power levels are mutually exclusive events. Hence,

$$\sum_{k=1}^{K} \alpha_k \leq 1 \tag{11}$$

where the equality holds when the channel is always occupied.

The left-hand side of equation 11 represents the probability that any of the K transmitters is active, i.e. the probability that the channel is occupied, and its complementary probability $1 - \sum_{k=1}^{K} \alpha_k$ is the probability that the channel is free. The PDF of the received average power, $f_R(P_R)$, will be that of the k-th primary signal (with noise), $f_{S_k}(P_{S_k})$, whenever the k-th transmission power is active (which will occur with probability α_k), or it will be thermal noise, $f_N(P_N)$, otherwise. Hence:

$$f_R(P_R) = \left(1 - \sum_{k=1}^{K} \alpha_k\right) f_N(P_N) + \sum_{k=1}^{K} \alpha_k \, f_{S_k}(P_{S_k}) \tag{12}$$

and the resulting expression for the DC becomes:

$$\begin{aligned} \Psi &= \int_{\lambda}^{\infty} f_R(P_R) dP_R = \left(1 - \sum_{k=1}^{K} \alpha_k\right) P_{fa} + \\ &+ \sum_{k=1}^{K} \alpha_k \, Q\left(\frac{Q^{-1}(P_{fa}) \, \sigma_N - \gamma_k}{\sigma_{S_k}}\right) \end{aligned} \tag{13}$$

where $\gamma_k = \mu_{S_k} - \mu_N$ is the SNR resulting from the k-th average transmission power level, expressed in decibels.

To validate equation 13, the same approach of section VI-B is followed. First, the parameters required for equation 13 are obtained measuring the system's thermal noise (μ_N, σ_N) and estimating the rest of parameters (μ_{S_k}, σ_{S_k}, α_k) by fitting equation 12 to the empirical PDF of the captured sequence. The number of transmitters K can readily be determined by counting the number of peaks in the empirical PDF others than that of the thermal noise. The validity of this approach is verified in Figure 7 (as opposed to Figure 6, in this case there are several transmitters in the channel). For the part of the empirical PDF corresponding to the thermal noise some divergence is observed between the empirical and fitted curves. This can be explained by the presence of ambient noise. The values of μ_N and σ_N employed in the fitting procedure are obtained by replacing the antenna with a matched load in order to measure the system's noise. In this case the ambient noise is not captured and the noise part of the fitted curve resembles that of the system's noise. However, when connecting the antenna, the signal captured when no primary transmission is active also includes the ambient noise, thus leading to a slightly higher noise level than when measuring with the matched load. In any case, the fitting for the rest of peaks of the empirical PDF (i.e., primary signals, denoted as $S_1, S_2, \ldots$) is shown to be satisfactory, indicating that primary signal parameters are estimated accurately. By applying these estimated parameters to equation 13, a theoretical DC curve is obtained. The empirical DC curve is obtained as in section VI-B and compared in Figure 7 to the theoretical DC curve. Since several primary signals are present with different SNR values each, the DC is shown in this case as a function of the SNR offset, i.e. the amplitude correction factor applied to the original sequence in order to obtain various SNR values. As it can be appreciated, the theoretical and empirical curves perfectly agree, thus validating equation 13.

VII. Applicability of the Model

The model proposed in this work is theoretical in essence and provides closed-form expressions that can be employed in analytical studies. However, the model is not restricted to analytical studies but it could find more practical applications.

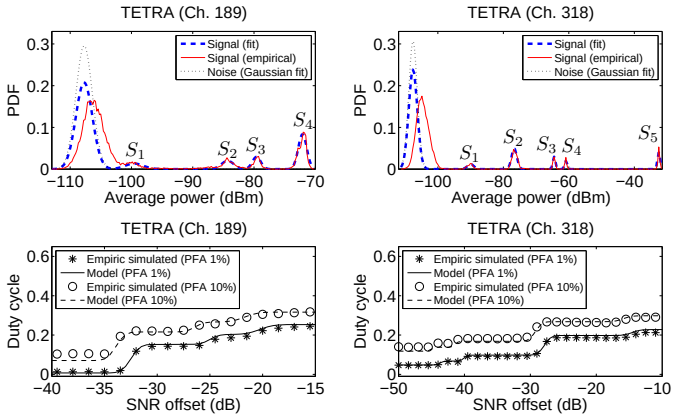

Fig. 7. Validation of the approach to estimate signal parameter's (upper part) and DC model for variable-power discontinuous transmitters (lower part).

One illustrative example is the simplification of simulation platforms. Let's assume two system level simulators integrated into a single simulation platform and working together. One of them emulates a whole primary network and is required to know what channels are actually occupied at any time instant during the simulation. This information is used by the second simulator, emulating a secondary CR network, to decide if the CR terminals at different locations observe the channels as occupied or not, and therefore if they transmit or remain inactive. The model proposed in this work can be used to replace the primary network simulator. Based on the locations of the primary transmitters, the knowledge of some basic signal parameters and the use of a propagation model, it is possible to determine the DC that would be perceived at each location inside the simulation scenario. This value can be thought of as the probability that each channel is observed as occupied at each location, and the local decisions of CR terminals can be obtained e.g. by comparing the DC value Ψ computed at their locations with a random value X_0 drawn from a uniform distribution $U(0,1)$. If $X_0 \leq \Psi$, then the CR terminal would observe the channel as occupied. Replacing the primary network simulator with this simulation model would result in a more efficient simulation platform and therefore in significantly reduced simulation times.

Another good example is the simplification of a spectrum measurement campaign in the context of CR as those performed in [1–6]. To obtain statistically accurate results on the occupancy level of various bands it is necessary to capture a sufficiently high number of data samples, which normally requires long measurement periods in the order of several hours even days. If the measurements are to be repeated at different locations, the measurement campaign might require several weeks/moths. Instead of performing a high number of long measurements sessions, it would be enough to perform a single long measurement at a high-position with direct line of sight to the transmitters of interest (high SNR conditions) in order to accurately estimate the AF of the desired transmitters, and then perform some relatively short measurement sessions at the locations of interest in order to obtain good estimates of the received power means μ_{S_k} and standard deviations σ_{S_k}. The model proposed in this work could then be applied to estimate the occupancy levels that would be observed at each location. Therefore, in order to measure the occupancy level of L locations, the model could be employed to reduce the overall measurement time from L long measurement sessions to only one long measurement session and L short measurement sessions. These are only some examples of the potential applications of the model proposed in this work.

VIII. Conclusions

Spectrum occupancy modeling in the context of DSA/CR constitutes a rather unexplored research area that still requires much more effort. This paper has addressed the problem of modeling spectrum occupancy in the spatial domain by proposing a novel theoretical approach that enables modeling the occupancy level perceived at any geographical location based on the knowledge of some simple primary signal parameters. The validity of the theoretical model has been verified with extensive empirical measurement results. Some examples of its potential applicability have been discussed as well.

Acknowledgements

This work was supported by the European Commission in the framework of the FP7 FARAMIR Project (Ref. ICT-248351) and the Spanish Research Council under research project COGNOS (Ref. TEC2007-60985). The support from the Spanish Ministry of Science and Innovation (MICINN) under FPU grant AP2006-848 is hereby acknowledged.

References

[1] M. A. McHenry *et al.*, "Spectrum occupancy measurements," Shared Spectrum Company, Tech. Rep., Jan 2004 - Aug 2005, available at: http://www.sharedspectrum.com.

[2] A. Petrin and P. G. Steffes, "Analysis and comparison of spectrum measurements performed in urban and rural areas to determine the total amount of spectrum usage," in *Proc. International Symposium on Advanced Radio Technologies (ISART 2005)*, Mar. 2005, pp. 9–12.

[3] R. I. C. Chiang, G. B. Rowe, and K. W. Sowerby, "A quantitative analysis of spectral occupancy measurements for cognitive radio," in *Proc. IEEE 65th Vehicular Technology Conference (VTC 2007 Spring)*, Apr. 2007, pp. 3016–3020.

[4] M. Wellens, J. Wu, and P. Mähönen, "Evaluation of spectrum occupancy in indoor and outdoor scenario in the context of cognitive radio," in *Proc. Second International Conference on Cognitive Radio Oriented Wireless Networks and Communications (CrowCom 2007)*, Aug. 2007, pp. 1–8.

[5] M. H. Islam *et al.*, "Spectrum survey in Singapore: Occupancy measurements and analyses," in *Proc. 3rd International Conference on Cognitive Radio Oriented Wireless Networks and Communications (CrownCom 2008)*, May 2008, pp. 1–7.

[6] M. López-Benítez, F. Casadevall, A. Umbert, J. Pérez-Romero, J. Palicot, C. Moy, and R. Hachemani, "Spectral occupation measurements and blind standard recognition sensor for cognitive radio networks," in *Proc. 4th International Conference on Cognitive Radio Oriented Wireless Networks and Communications (CrownCom 2009)*, Jun. 2009.

[7] I. F. Akyildiz, W.-Y. Lee, M. C. Vuran, and S. Mohanty, "NeXt generation/dynamic spectrum access/cognitive radio wireless networks: A survey," *Computer Networks*, vol. 50, no. 13, pp. 2127–2159, Sep. 2006.

[8] D. Willkomm, S. Machiraju, J. Bolot, and A. Wolisz, "Primary users in cellular networks: A large-scale measurement study," in *Proc. 3rd IEEE Symposium on New Frontiers in Dynamic Spectrum Access Networks (DySPAN 2008)*, Oct. 2008, pp. 1–11.

[9] M. Wellens, J. Riihijärvi, and P. Mähönen, "Spatial statistics and models of spectrum use," *Elsevier Computer Communications*, vol. 32, no. 18, pp. 1998–2011, Dec. 2009.

[10] M. López-Benítez and F. Casadevall, "Methodological aspects of spectrum occupancy evaluation in the context of cognitive radio," in *Proc. 15th European Wireless Conference (EW 2009)*, May 2009, pp. 199–204.

[11] ——, "On the spectrum occupancy perception of cognitive radio terminals in realistic scenarios," in *Proc. 2nd International Workshop on Cognitive Information Processing (CIP 2010)*, Jun. 2010, pp. 1–6.

[12] T. Yücek and H. Arslan, "A survey of spectrum sensing algorithms for cognitive radio applications," *IEEE Communications Surveys and Tutorials*, vol. 11, no. 1, pp. 116–130, 2009.

[13] D. D. Ariananda, M. K. Lakshmanan, and H. Nikookar, "A survey on spectrum sensing techniques for cognitive radio," in *Proc. of the Second International Workshop on Cognitive Radio and Advanced Spectrum Management (CogART 2009)*, May 2009, pp. 74–79.

[14] A. Papoulis and S. U. Pillai, *Probability, random variables, and stochastic processes*, 4th ed. Boston: McGraw-Hill, 2002.